Mechanical behaviour and durability of high volume fly ash cementitious composites

Usman Haider, Zdeněk Bittnar, Lubomír Kopecky, Petr Bittnar, Jiří Němeček
Department of Mechanics, Faculty of Civil Engineering, Czech Technical University in Prague, Czech Republic
usmanhaider6886@gmail.com

Asif Ali
Department of Chemical Engineering, University of Engineering and Technology, Lahore, Pakistan

Jaroslav Pokorny
Department of Material Engineering and Chemistry, Faculty of Civil Engineering, Czech Technical University in Prague, Czech Republic

ABSTRACT. The purpose of this research is to separate different morphological particles of ASTM class F fly ash, and study their effect on mechanical behaviour and durability of high volume cementitious mixtures. In this research wet separation of raw fly ash is carried out, which resulted in three layers of different morphological particles. The first layer of particles float, comprise of about 1-5% of fly ash, is identified as cenospheres or hollow spheres. The second layer of particles is measured to be 55-60% of raw fly ash and consisting of porous spherical and rounded particles rich in Si and Al. The third layer particles is measured to be about 35-40% of raw fly ash. High volume fly ash cementitious composites containing second or third layer particles are tested under compression and bending, highlighting a higher strength and ductility in comparison to cementitious ones containing raw fly ash particles.

KEYWORDS. Cementitious matrix; Raw fly ash; Second layer particles; Third layer particles.

Citation: Haider, U., Bittnar, Z., Kopecky, L., Bittnar, P., Němeček, J., Ali, A., Pokorny, J., Mechanical behaviour and durability of high volume fly ash cementitious composites, Frattura ed Integrità Strutturale, 38 (2016) 289-302.

Received: 23.04.2016
Accepted: 15.07.2016
Published: 01.10.2016

INTRODUCTION

Fly ash produced from combusting coal is generated in excess of 750 million tons globally and at current coal combustion rate the world coal reserves will still last for about 150 more years [1-2]. Landfilling of fly ash was considered a viable solution, but new legislations in the world are increasing the costs of landfills. Thereby energy companies are themselves encouraging the research on fly ash not, only to reutilize the everyday produced fly ash, but as

well as to reuse the already disposed fly ash [3]. Fly ash, which used to be known as a waste, is recognized as a useful chemical substance and it is a REACH registered product, having several useful applications [4-7]. There are about 861 billion tonnes of coal reserves in the world of which half consists of brown coal deposits [8-9].
Morphology of fly ash is highly affected by the source of pulverised coal and amount of water present in the pores of the coal particles, which are combusted to produce it [10]. Morphology of fly ash consists of pseudo spheres and irregular particles containing: aluminium, silicon, calcium, iron, carbon from unburned coal, and lesser abundance of other twenty six elements, mostly consisting of heavy metals and some rare earth elements [11-12].
Different morphological and rich chemical composition possessed by fly ash are a hurdle for its own utilization in certain applications, where one part of it is more desirable than others, which can be resolved by separating its particles by some technique [13]. Therefore, separation of particles of fly ash is required in finding new applications.
Various studies have been carried out to extract and analyse hollow spheres which float on the surface of water, when wet separation methods are employed. Kolay and Singh [14] and Ngu et al. [15] carried out studies on physico-chemico-mineralogical properties of hollow spheres recovered from surface of fly ash lagoons, separated by water. They showed the presence of oxides of Si, Al, and Fe to be between 50-60%, 30-35%, and 5-10% respectively. Kolay and Bhusal [16] obtained cenospheres / hollow spheres of two different densities by wet separation using water and Lithium Metatungstate solution, the later employed in order to recover some percentage of hollow spheres even contained in the sinked part during water separation.
Such microspheres represent about 70 to 75% of fly ash, depending on: origin of coal, combustion method, and cooling rate [17]. Over of these microspheres, hollow spheres, which have densities less than water, are recovered from top of water surface by sink float method. About 1-5% of the fly ash is hollow spheres [17-18].
ASTM C618 classifies fly ashes according to their chemical composition in two types: Class C and Class F [19]. Class C fly ashes are characterized by the fact that when added to water react and rapidly harden, whereas this phenomenon is not observed for Class F fly ashes [16]. The later type is characterised by a separation of its particles based on their densities, when mixed in water.
It is well known that finer and amorphous materials are able to accelerate the pozzolanic reaction in order to improve the strength characteristics of mortars and concretes [20]. The pozzolanic reactivity of pulverized coal fly ash is due to the presence of active silica and alumina, which initiates pozzolanic reaction by reacting with calcium hydroxide, derives from cement hydration [21].
However due to larger size of raw fly ash particles as compared to cement particles, concrete and mortar strength is not significant increases if high volume fly ash is used. Therefore, efforts are made in order to obtain finer particles, such as for example air classifier systems [22] or wet separation systems. Usually with the air classification methods two types of products are obtained: underflow and overflow products, or coarse and fine products [23]. Air classifiers have some drawbacks [24]. Firstly, the percentage of overflow / fine products recovered is very low, while significant percentages of underflow / coarse products are produced simultaneously [25]. Secondly, the yield of overflow / fine products is very low. Thirdly, the cost of air classification machines is considerably high [25].
The strength and durability of cementitious structures are important properties since they define the service life of the structure [26]. As a matter of fact, finer particles of fly ash, due to their smaller particle size and larger surface area, have the ability to increase strengths and increase long-term durability in cementitious materials [27]. Studies regarding effects of fly ash on strength and durability of cementitious structures are available in literature [28-30]. The use of fly ash to replace cement in cementitious materials reduces the consumption of cement and thereby reduces CO_2 emissions related to cement production [31, 32]. Fly ash has several uses, but still its global utilization is 25% of the world's fly ash production [33]. However, there are some obstacles for utilizing fly ash in large volumes in cementitious composites, such as slow development of strength, quality and composition of fly ash, setting time issues etc. [34]. Furthermore, it is not clearly known how ASTM Class F fly ashes affect strength, and resistance to ingress of chemical when added in large volumes in cementitious materials.
Most of the studies that have been carried out on wet separation of ASTM Class F brown coal fly ash using water focus on the hollow spheres, which float on the water surface being a minute fraction of the particles in fly ash. A detailed physical, morphological, chemical, and mineralogical analysis on remaining 95-99% of the fly ash which sinks in water after wet separation is not available in the literature. Therefore, the purpose of this research is to carry out wet separation of ASTM Class F brown coal fly ash using water and then examine the physical, morphological, chemical, and mineralogical properties of the separated parts of raw fly ash. Then, the paper is focussed on strength and durability of high volume cementitious mixtures when some types of the above parts are added to the mixture.

EXPERIMENTAL CAMPAIGN

Separation method

ASTM Class F brown coal raw fly ash produced by Počerady power plant of Czech Republic was used to carry out wet separation. Initially, 600 ml of water was added to a graduated 1000 ml glass cylinder followed by 400 grams of raw fly ash, making up a total volume of 800ml. After this, the resulting mixture was well shaken for about fifteen minutes manually and left at room temperature for duration of 4 hours. After such a time, three distinct layers of raw fly ash solution were observed, as shown in Fig. 1. The particles of first layer were greenish grey in colour, including black particles which floated on the surface and comprised of about 10ml volume. Clear water of about 400ml was observed. The second layer is comprised of 250ml volume of greyish green particles of raw fly ash, and third layer is comprised of greyish black particles of 150ml volume. It was seen from the results of tests carried out that second and third layer varied from 40 to 60% of the volume.

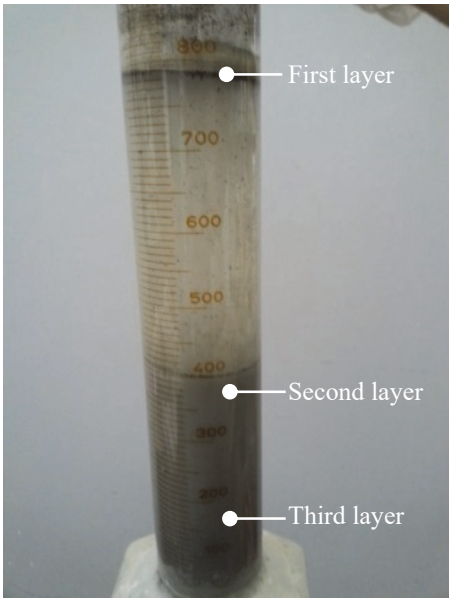

Figure 1: Wet separation of raw fly ash in laboratory.

Tests to determine physical properties

Particle size analysis of raw fly ash and separated fly ash particles were carried out on Fritsch Analysette 22, a laser particle size analyser, using its wet dispersion unit. Density of raw fly ash, and its separated parts, was determined using helium Pycnometer, Pycnomatic ATC. Specific surface areas of raw fly ash, and its separated parts, were measured using BET method on PC-controlled volumetric gas-adsorption system Sorptomatic 1990.

Optical images of particles were observed by using a Zeiss (Germany) Axio Imager optical microscope.

Mercury intrusion porosimetry tests were carried out to measure the porosity of cementitious samples using Pascal 440 Porosimeter manufactured by Thermo scientific (USA).

For moisture content determination, the cementitious specimens were fully saturated by fully immersing in water under vacuum for 24 hours. After fully saturating the specimens they were placed in the oven at 50^{o} C and were weighed at 1, 2, 7, 14, and 30 days to check the moisture difference.

Tests to determine morphological properties, chemical composition and mineralogical properties

In order to determine morphology of raw fly ash and its separated particles, images were captured by HE-SE detector on Merlin Carl Zeiss (Germany) field emission electron microscope (FE-SEM). Large / total area analysis were carried out to by using rectangular selection tool in EDX software AZtecEnergy in order to determine overall chemical composition up to thirty elements.

Small area and point analysis were carried out by using point and irregular area selection tools in EDX software AZtecEnergy to determine chemical composition of thirty elements both in the individual raw fly ash and separated fly ash particles.
Regarding the X-ray Diffraction (XRD) analysis used to determine the mineralogical composition; X-ray powder diffraction data were collected at room temperature with a Bruker AXS D8 θ-θ powder diffractometer with parafocusing Bragg-Brentano geometry using CoK_{α} radiation (λ = 1.79021 Å, U = 34kV, I = 30 mA).

Tests to determine mechanical properties

Specimens of size 40 x 40 x 160 were prepared for flexural strength testing in accordance with ČSN ISO 4013 [35], by employing a cement replacement of 60% by weight of raw fly ash, or second layer particles, or third layer particles at water to cement ratio of 0.4. For compression, half-broken specimens from flexure test were used in accordance with ČSN ISO 1920 [36]. Mixture was prepared in accordance with ČSN EN 480-1 [37] and, after preparation, specimens were cured in an environmental chamber at a constant temperature of 22°C, with relative humidity of 50% up to 90 days. During flexural testing, load and deflection of the specimens were measured. Vicat apparatus was used to carry out measurements of compliance by means of setting time measurements in accordance with ČSN EN 196-3 [38].

Tests to determine the mixture behaviour under harsh environments

Non-standardized rapid chloride penetration tests were carried out to determine the mixture behaviour under harsh environments which is slightly different from that of ASTM C1202 [39]. The apparatus of this test consisted of electro-migration chamber with two compartments filled with a 3% NaCl solution on the negative end and with 0.3 M NaOH solution on the positive end.

RESULTS AND DISCUSSION

Physical properties

As is well known, particle size indicates performance and quality of powders, suspensions, emulsions, and aerosols and has strong influence on mechanical properties of concrete [40]. Therefore particle size distribution (Fig. 2) was carried out to determine the measures of central tendency. Median diameter, d_{50}, is regarded as a useful measure in comparing particle sizes of distributions. Tab. 1 shows that particles of second layer are finer than raw fly ash and third layer, but coarser than cement particles, whereas third layer particles are the coarsest.

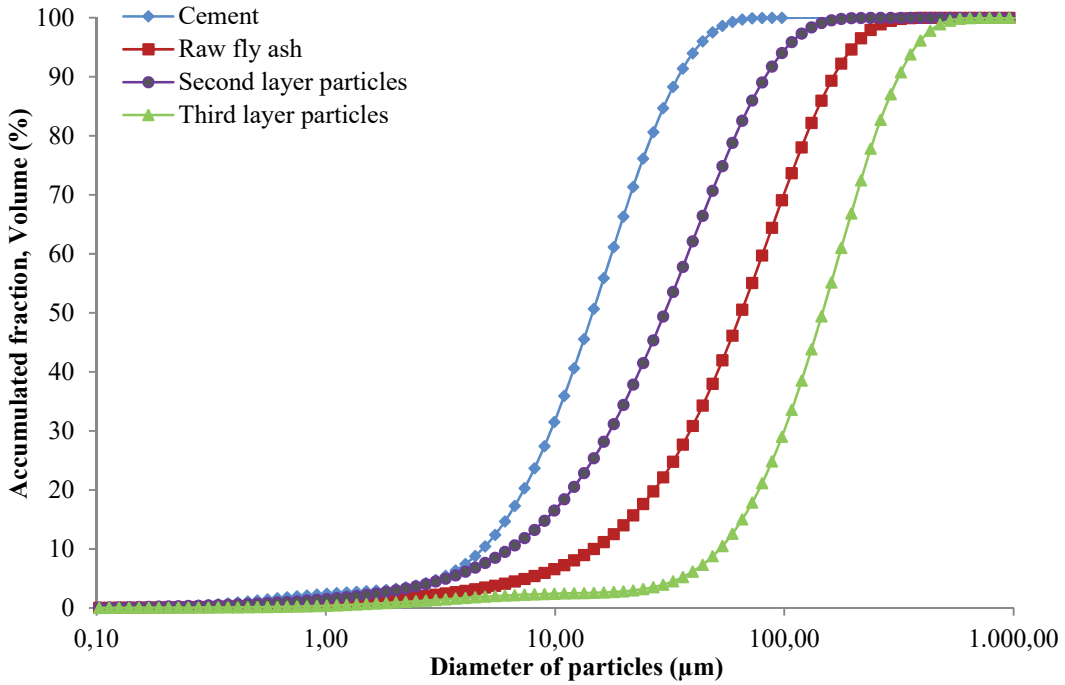

Figure 2: Cumulative particle size distribution comparison: cement, raw fly ash, second layer particles, and third layer particles.

Upper limit diameter, d_{97}, listed in Tab. 1, is a useful measure to determine the upper limit of particle size distribution and is used by industries dealing with powdery materials [41]. The table shows that d_{97} of second layer is lesser than that of raw fly ash and third layer, but larger than that of cement, which is an indication that second layer particles are finer for even the upper limit of particle sizes. Comparison of densities for cement, raw fly ash, second layer, and third layer is also presented in Tab. 1, which shows that cement has the highest density followed by third layer, raw fly ash, and second layer. Density of raw fly ash is more than second layer and lower then third layer, but closer to the second layer, which indicates that second layer particles are present in larger quantity in raw fly ash, nearly 55-60% against the 35-40% of the third layer particles. Specific surface areas of raw fly ash, second layer, and third layer presented in Tab. 1, showing that second layer particles have 100% larger specific surface area compared to that of raw fly ash particles, and 73% larger specific surface area compared to cement particles. Therefore, second layer particles have lesser particle size, lesser density, and more specific surface area as compared to raw fly ash and third layer particles.

Particle type	Median diameter, d_{50} (μm)	Upper limit diameter, d_{97} (μm)	Density (g/cm^3)	Specific surface area (cm^2/g)
Cement	14.6	47.0	3.1	22000
Raw fly Ash	60.1	230.7	2.2	19000
Second layer	32.2	110.3	1.9	38000
Third Layer	146.7	413.3	2.7	9000

Table 1: Physical properties of particles.

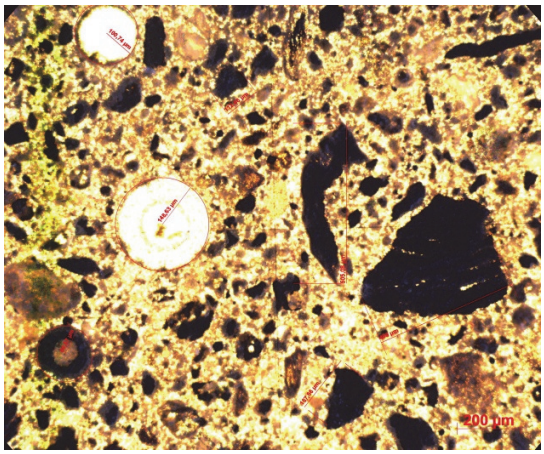

(a) Raw fly ash

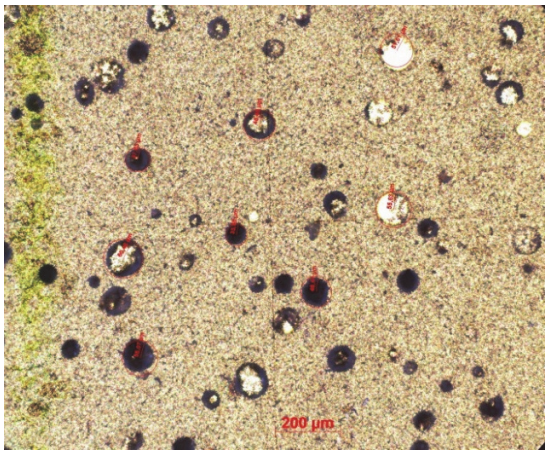

(b) First layer

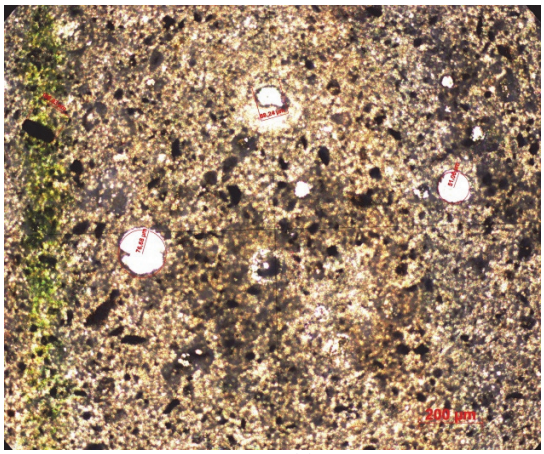

(c) Second layer

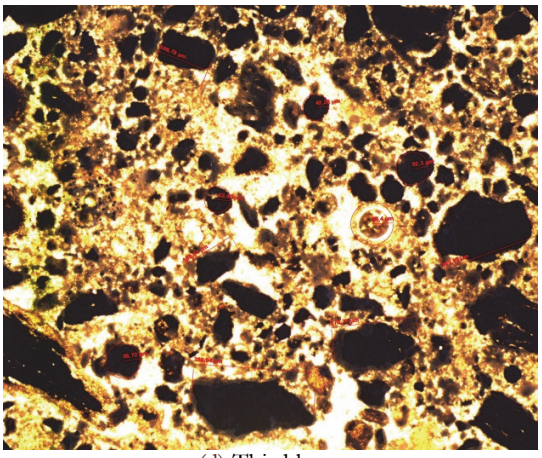

(d) Third layer

Figure 3: Optical images of: raw fly ash (a), first layer (b), second layer (c), and third layer particles (d) at 10 X magnification.

Optical microscopic images were observed at 10 X magnification as shown in Fig. 3. As it can be noted in Fig. 3(a) raw fly ash particles consist of solid spherical, hollow spherical, and slaggy particles of various sizes ranging from 7.6 to 16.7 μm, 23.8 to 148 μm, and 63 to 505 μm, respectively. The first layer particle (Fig 3(b)) consists of mostly hollow spheres of sizes varying from 20 to 80 μm, whereas few solid spherical particles of almost the same size as hollow spherical particles. First layer particles are well known as cenospheres [42]. The second layer particles (Fig. 3(c)) consist of very fine rounded slaggy particles of size 8 to 30 μm, spherical particles of size 5 to 40 μm, and few hollow spherical particles of size 70 to 158 μm. The third layer particles (Fig. 3(d)) consists of mostly compact slaggy particles of measured sizes ranging from 27.2 to 566 μm, and few solid spherical particles of measured sizes 15.1 to 77.4 μm.

To determine the porosity in each specimen it is necessary to determine the type of pores that exist in the hydrated cementitious specimens. Mercury intrusion porosimetry is well known method to determine pore size distribution of specimens and it was carried out to determine porosity of raw fly ash, second layer, and third layer cementitious specimens as shown in Fig. 4(a). Fig. 4(b) shows differential pore size distribution curves which are obtained by differentiating the curves in Fig. 4(a). In Fig. 4(b) it can be seen that samples containing raw fly ash, second layer, and third layer particles show the maximum concentration of pores at critical diameters of 0.065, 0.055, and 0.022 μm with differential peak volumes of 0.011, 0.018, and 0.011 cm^3/g.

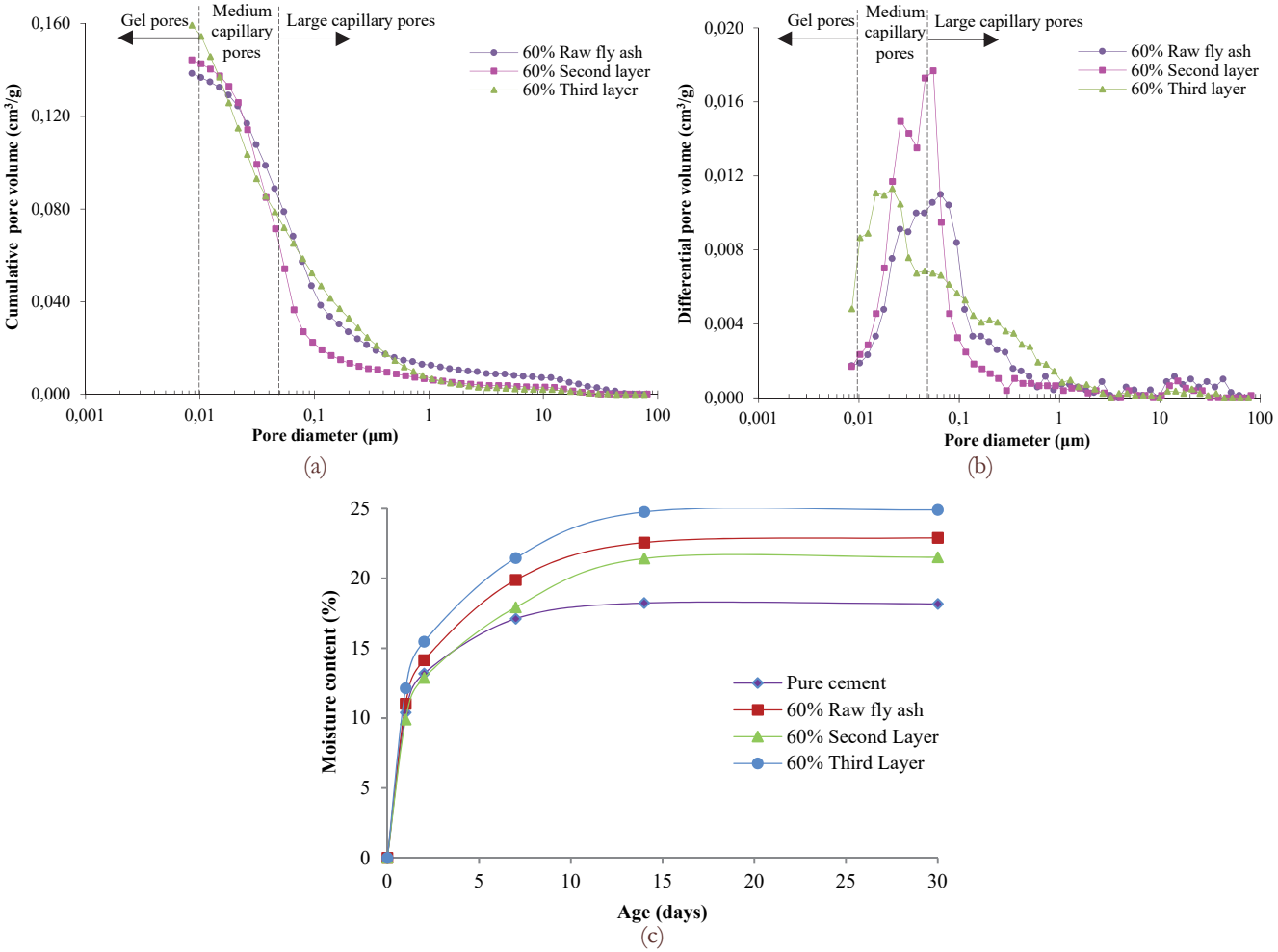

Figure 4: Mercury intrusion porosity, cumulative pore volume vs pore diameter (a), incremental / differential pore volume vs pore diameter (b), and moisture content vs age of specimens (c).

Fig. 4(c) shows the moisture content exuded/discharged by the fully saturated specimens of raw fly ash, second, and third layer while in the oven. It can be seen in such a figure that as the age of drying is increased for fully saturated specimens, moisture is rapidly exuded by the specimens and after 14 days of drying the moisture curves are seen to be flat which means all moisture is discharged up to 14 days. It is seen here as well that specimens containing third layer particles

exuded more moisture as compared to specimens having raw fly ash and second layer particles in them, because second layer particles are more tightly packed due to smaller particles, larger surface area, and spherical shape of particles [43].

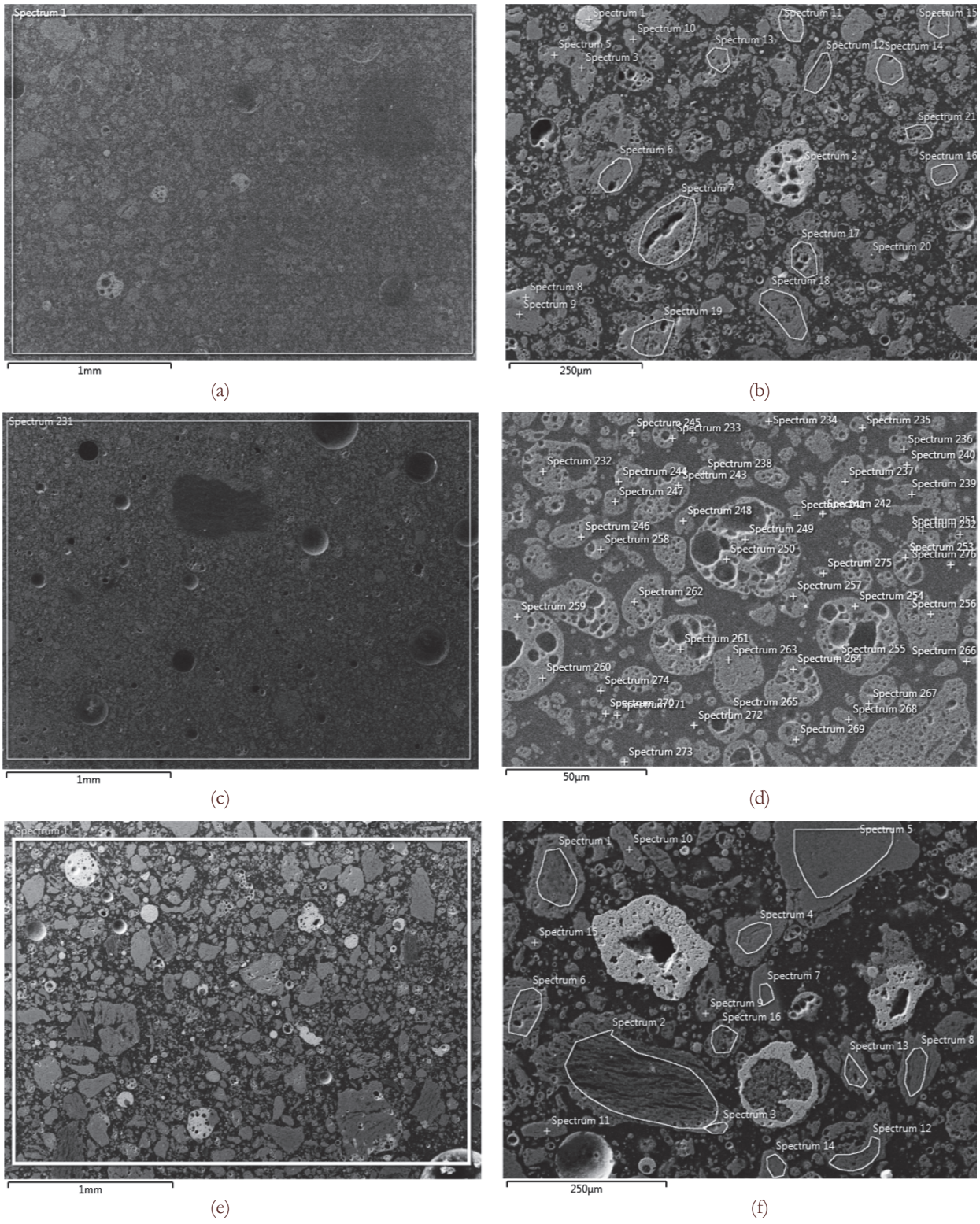

Figure 5: Energy Dispersive X-ray Spectrometry (EDX) large area analysis for: raw fly ash at 75 X magnification (a) and at 500 X (b); second layer at 75 X magnification (c) and at 1.5 KX (d); third layer at 75 X magnification (e) and at 500 X magnification (f).

Morphological properties, chemical composition and mineralogical properties

Field emission electron microscope was used to determine the morphology of individual submicron and ultrafine particles present in the raw fly ash, second layer, and third layer particles (Fig.5). From FE-SEM images in Fig. 5(a) and (b) it can be observed that raw fly ash consists of micron, submicron and ultrafine size particles. FE-SEM images in Fig. 5(c) show that second layer particles consists of majority of submicron and ultrafine (<1μm) particles. In Fig. 5(d) submicron to ultrafine (<1μm) size particles can also be observed. Fig. 5(e) shows FE-SEM images of third layer particles consisting in much bigger in size as compared to those of second layer particles. In Fig. 5(f) it can be seen that particles of third layer contain significant amount of bright particles [44], which are absent in the images of second layer. FE-SEM images of Fig. 5(a), (c), and (e) were carried out in which maximum area at lowest possible magnification was covered in electron microscope in order to determine chemical composition of specimens, listed in Tab. 2.

Tab. 3 shows that Amorphous, quartz (SiO_2), mullite ($Al_{0.69}\,Si_{1.22}\,O_{4.85}$), and magnetite ($Fe_3O_4$) phases are present in raw fly ash, second layer, and third layer.

	Al	Si	K	Ca	Ti	Fe	Na	Mg	P	Zr
Raw fly ash	26.18	60.81	2.09	1.34	0.89	1.35	1.54	1.39	0.00	3.63
Second layer	25.97	60.29	3.19	1.88	0.96	0.93	0.74	0.72	0.83	2.71
Third layer	25.25	53.77	4.06	2.36	1.58	8.89	0.63	1.11	0.33	0.53
	Ba	Bi	S	V	Cr	Mn	Co	Ni	Cu	Zn
Raw fly ash	0.00	0.29	0.00	0.00	0.00	0.03	0.00	0.06	0.07	0.13
Second layer	0.07	0.00	0.21	0.22	0.10	0.00	0.14	0.00	0.00	0.05
Third layer	0.00	0.00	0.22	0.08	0.00	0.17	0.00	0.01	0.03	0.14
	Ga	Ge	As	Se	Rb	Sr	Y	La	Ce	Hg
Raw fly ash	0.11	0.03	0.00	0.05	0.30	0.00	0.00	0.00	0.00	0.00
Second layer	0.03	0.02	0.00	0.25	0.18	0.01	0.12	0.00	0.00	0.00
Third layer	0.02	0.00	0.00	0.00	0.00	0.00	0.00	0.09	0.00	0.25

Table 2: Chemical composition from Energy Dispersive X-ray Spectrometry (EDX) analyses for raw fly ash, second layer particles, and third layer particles.

Specimen	Amorphous (%)	Quartz (%)	Mullite (%)	Magnetite (%)
Raw fly ash	40	19	39	2
Second layer	45	17	37	1
Third layer	37	18	38	7

Table 3: X-ray Diffraction (XRD) mineralogical composition of raw fly ash, second layer particles, and third layer particles.

Using EDX analyses, individual particles in raw fly ash of Fig. 5(b) were analysed with small area and point analyses for the composition of Si, Al, Fe, Ca and other twenty seven elements present in them.

Ternary Si-Al-Fe diagram for raw fly ash, second layer, and third layer particles are shown in Fig. 6(a) - (b). Similarly ternary diagrams were plotted to compare the ratio of percentages of Si, Al, and Ca for raw fly ash, second layer, and third layer particles as shown in Fig. 6(c) - (d). Fig. 6(e) and (f) shows ternary diagram between Alkali and Alkaline metals (AAM), metalloids and non-metals (MNM), and transition heavy metals (THM) in particles of raw fly ash, second layer, and third layer particles.

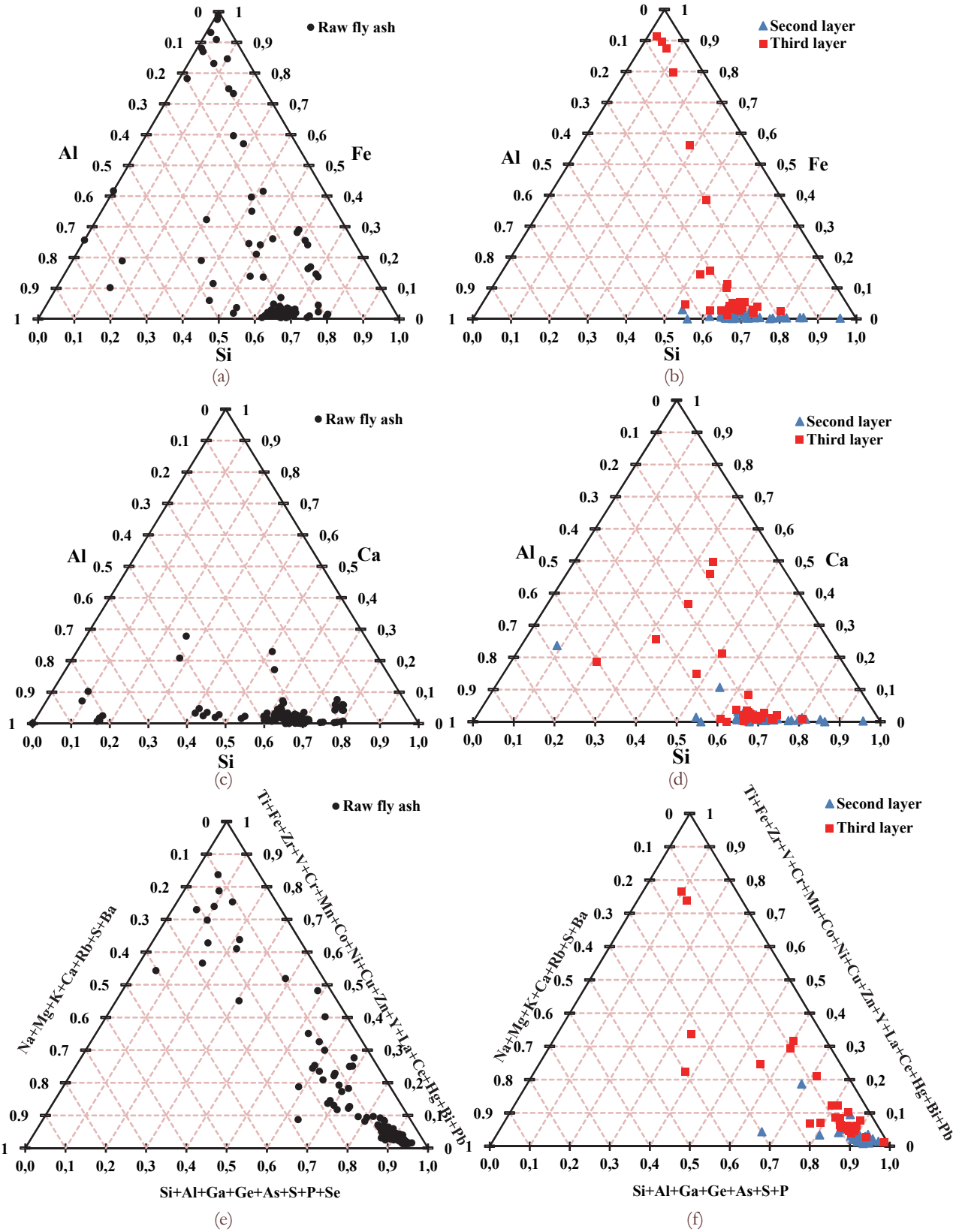

Figure 6: Ternary diagrams from Energy Dispersive X-ray Spectrometry (EDX) analyses between: Si – Al – Fe for raw fly ash (a), second and third layer particles (b); Si – Al – Ca for raw fly ash (c), second and third layer particles (d); between Alkali and Alkaline Metals – Metalloids and Non-Metals – Transition Heavy Metals for raw fly ash (e), second and third layer particles (f).

Mechanical properties

Specimens were prepared with 60% cement replaced with raw fly ash, 60% cement replaced with second layer, and 60% cement replaced with third layer. Specimens prepared with pure cement developed cracks due to high heat of hydration and gave inappropriate results: therefore their results are not included in this paper. Flexural and compressive strengths were tested at 7, 14, 28, and 90 days as shown in Fig. 7(a) and (b). Load-deflection relationships were developed for specimens at 90 days only as shown in Fig. 7(c). Fig. 7(a) shows that as the age of specimens increase, flexural strength of all three types of samples increase. However the flexural strength increase for third layer particles is 20% more than that of raw fly ash, and second layer particles. The reason for 20% more flexural strength of third layer particles can be attributed to the compact angular fibre type morphology of third layer particles which resist flexural load more than spherical particles [45-46]. The reason of trend of strength curve of second layer is due to its glassy particles rich in active silica and amorphous content which produces more hydration products as compared to raw fly ash and third layer particles.

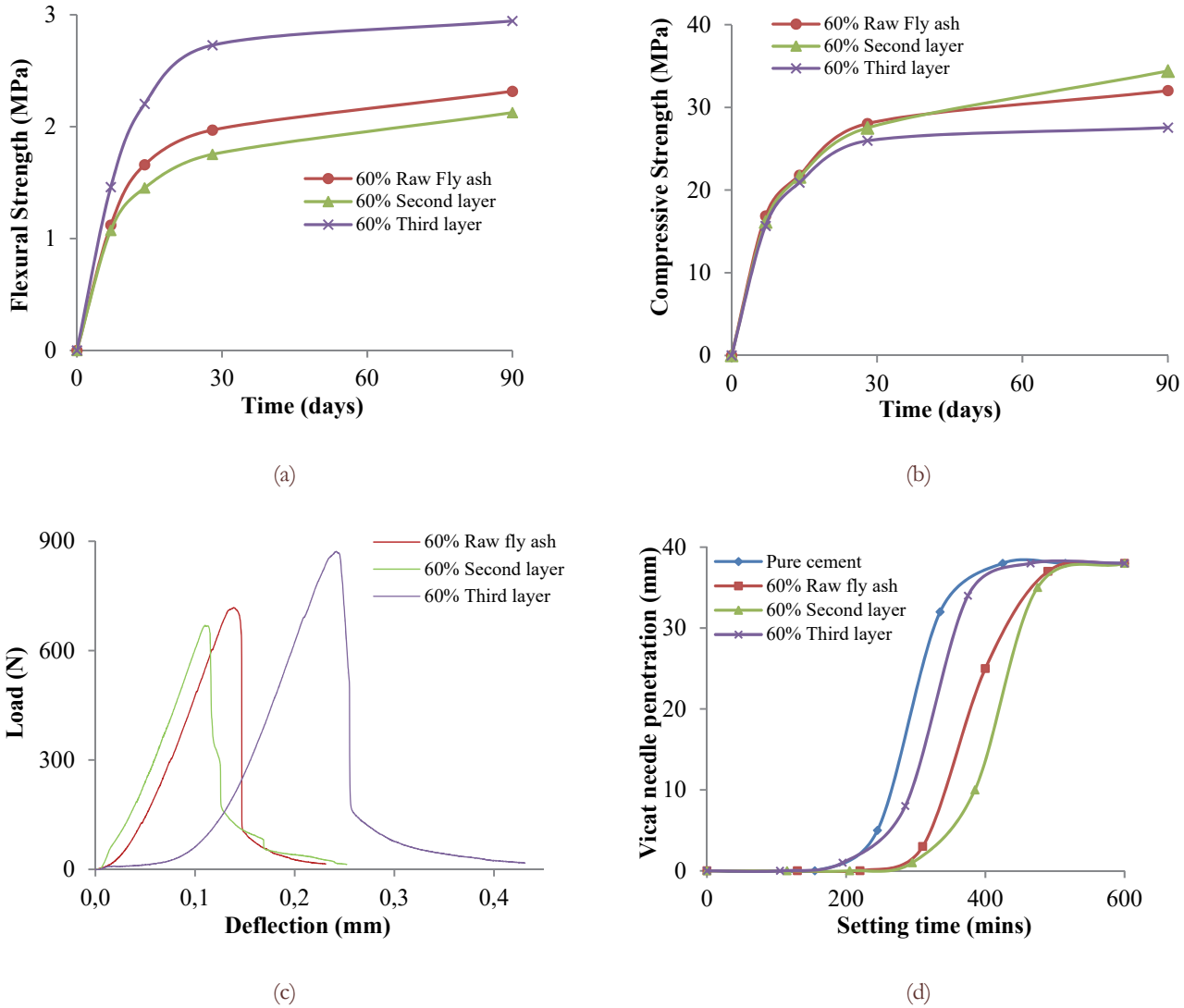

Figure 7: Flexural strength (a), compressive strength (b), load deflection curve (c) for cementitious: raw fly ash, second layer particles, and third layer particles; and setting time determination by vicat apparatus for cement, raw fly ash, second layer, and third layer particles (d).

It can be seen from Fig. 7(b) that as the age of all cementitious samples increase the compressive strength increases. Till 14 days age of specimens, much differences in compressive strengths are not seen for all the specimens. However as the age of specimen's increases, the compressive strength curve for second layer becomes steep and shows that hydration of second layer particles continue to produce additional C-S-H gel which gives 7% more compressive strength to it at the age of 90 days, as compared to raw fly ash particles. Whereas it can also be seen that hydration of particles of third layer slows down and its samples show less compressive strength at the age of 28 and 90 days as compared to raw fly ash and second layer samples. The reason for strength gain of samples as age of specimens increase is because in the mixtures as the cement particles start reacting with water and they produce calcium silicate hydrates and calcium hydroxides while silica and alumina in raw fly ash, second, and third layer particles react with calcium hydroxide to form additional calcium silicate hydrates and calcium aluminate hydrates which starts to give strengths mainly at and after 28 days [20-21]. However, the reason for which samples containing second layer particles show more compressive strength is because second layer particles have small particle size and large surface area which makes them reacts abruptly in cementitious mixtures to produce hydration products as compared to samples containing raw fly ash and third layer particles.
Fig. 7(c) shows load - deflection relationship when the specimens are tested in flexure at 90 days. Here it can be seen that samples of third layer particles have more flexural load taking ability and deflect more as compared to raw fly ash and second layer particles. The reason of this is because angular particles of third layer create better interlocking between particles which improves the strength and therefore large deformations occur [47].
Fig. 7(d) shows the curves between vicat needle penetration and setting time of paste for pure cement, 60% raw fly ash replaced with cement, 60% second layer replaced with cement, and 60% third layer replaced with cement. It can be seen here that vicat needle penetration which is an indication of the hardening or setting of cementitious pastes [48] is seen to be lowest with time for cement paste, which indicates that initial and final setting times of cement is lower than that of raw fly ash, second layer, and third layer containing cementitious pastes. Whereas third layer paste show lower setting time as compared to raw fly ash and second layer but more setting time as compared to cement paste. Second layer particles show more setting time as compared to cement, third layer, and raw fly ash pastes. The reason for increase of setting times of raw fly ash paste mixture as compared to cement paste mixture is that when the raw fly ash is replaced with cement, the concentration of cement particles decrease and the distance between the particles of cement increase, along with it lesser hydration products are formed, so both factors contribute to an increase in the setting time of raw fly ash paste mixture [49]. Whereas second layer comparatively finer particles fill in the voids between the cement particles and decrease further the concentration of cement in the second layer paste mixture and thus increase the setting time more as compared to raw fly ash paste [50]. The third layer particles have relatively large size of particles which lack finer particles in them and replacing cement with third layer particles in third layer cementitious paste firstly decreased the concentration of cement particles as compared to pure cement paste sample but cement also filled in the pores within third layer particles and cement concentration increased as compared to raw fly ash particles therefore as compared to raw fly ash paste third layer paste show decrease of setting time.
Further it can be seen in Fig. 7 that raw fly ash specimens showed properties that were closer to the second layer samples as compared to the third layer samples because raw fly ash particles, as seen in Fig. 1, were found to contain up to about 55-60% second layer particles and up to 35-40% third layer particles.

Behaviour under harsh environment

Fig 8 shows the graph between charge passed through a 50 mm cementitious sample vs time measured, when the specimens were exposed to 3% NaCl and 0.3 M NaOH solution on the negative and positive ends of a 20 V DC supply. It can be seen here that as the time increased from 0 to 48 hours, more charge passed through all the samples. However in 48 hours the charge passed through the third layer samples was the highest and lowest charge passed was recorded through second layer samples as compared to samples containing raw fly ash particles. The high permeability of samples containing third layer particles seen in Fig. 8(a) is due to the fact that the third layer particles contains very large angular particles, in which small size rounded particles are missing and when angular particles are packed together they create porosity in them. However, the second layer particles are more rounded particles which pack more tightly together and thus lesser charge passes through them as compared to samples having third layer angular particles [43]. Chloride concentration profiles per gram of the specimens are plotted versus their average depths in Fig. 8(b). Here it can be seen that samples containing third layer particles show high concentration of chlorides at depths between 2.5 and 17.5 mm as compared to samples containing raw fly ash and second layer particles. It is further seen that chloride penetrates the third layer particles till the depth of 17.5mm, whereas in samples having raw fly ash and second layer particles chlorides penetrate till depth of 12.5mm.

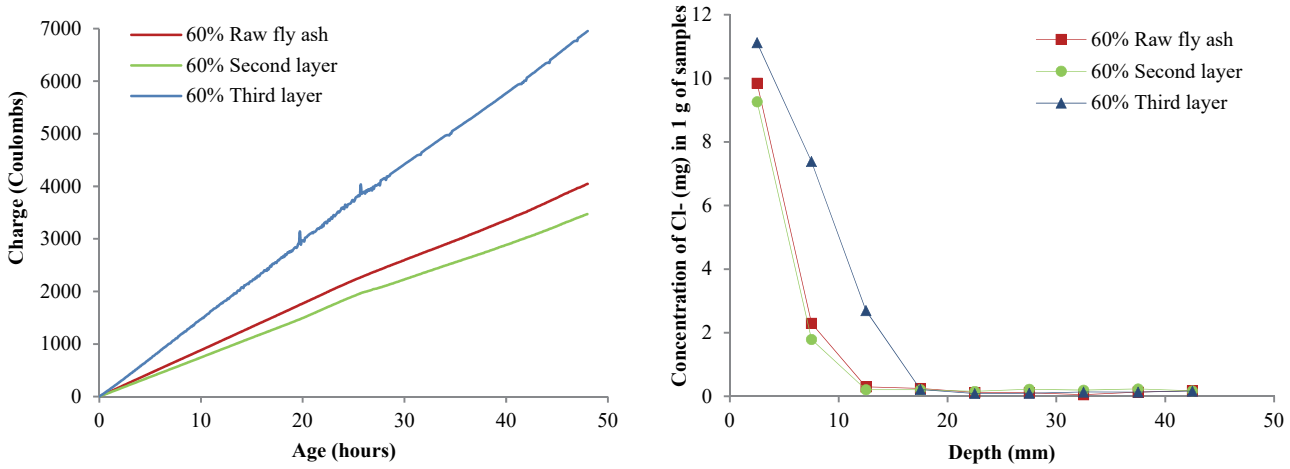

(a) (b)

Figure 8: Charge passed vs age of specimens (a), and chloride concentration vs depth of penetration (b).

Conclusion

In this research wet separation of brown coal raw fly ash from Počerady power plant of Czech Republic was carried out using water. Physical, morphological, chemical properties of separated parts were tested, and mechanical behaviour, durability in high volume cementitious mixtures were tested which leads to the following conclusions:

1. Three layers of raw fly ash were formed as it was added and mixed in water; particles of first layer which floated on the surface of water constituted of only about 1-5% of raw fly ash.
2. Second layer of particles were found to be finer particles as compared to raw fly ash. They consisted of mostly porous glassy spherical and rounded particles of submicron to ultrafine size rich in Si and Al while having very less contents of Fe in them.
3. The cementitious mixtures of second layer particles showed 7% increase in compressive strength as compared to raw fly ash cementitious mixtures and cementitious second layer specimens showed lesser chloride permeability and more resistance to ingress of chlorides.
4. Third layer particles were found to be coarse particles as compared to either second layer or raw fly ash particles. Morphologically third layer particles consisted of compact and large slaggy particles of several hundred microns size, rich in Si, Al, Fe, and heavy transition metals.
5. Cementitious mixtures of third layer particles showed 20% more flexural strength with large deformations as compared to cementitious mixtures of raw fly ash particles. Compressive strength was reduced and penetration of chlorides was found to be more as compared to raw fly ash.

Acknowledgement

The authors would like to thank Buildings and Settlement Information Modelling, Technology and Infrastructure for Sustainable Development under the project TE 02000077 by TAČR for providing funding for this research.

References

[1] Blissett, R.S., Rowson, N.A., A review of the multi-component utilisation of coal fly ash, Fuel, 97 (2012) 1–23. DOI: 10.1016/j.fuel.2012.03.024.
[2] Nicholls, T., How the Energy Industry Works: An Insiders' Guide, Silverstone Communications Ltd., London (2009) 111–112.
[3] Cez Group, http://www.cez.cz/en/power-plants-and-environment/coal-fired-power-plants.html, (2015).

[4] Punta, E., Lövgren, L., Ash is a useful chemical substance - It is registered in the European Chemical Register, http://www.varmeforsk.se/files/program/askor/2_puunta_.pdf, (2015).
[5] González, A., Navia, R., Moreno, N., Fly ashes from coal and petroleum coke combustion: current and innovative potential applications, Waste Manage Res., 27 (2009) 976–987. DOI: 10.1177/0734242X09103190.
[6] Zha, F., Liu, S., Du, Y., Cui, K., Behaviour of expansive soils stabilized with fly ash, Nat Hazards, 47 (2008) 509–523. DOI: 10.1007/s11069-008-9236-4.
[7] He, Y., Cheng, W., Cai, H., Characterization of α-cordierite glass–ceramics from fly ash, Journal of Hazardous Materials, 120 (2005) 265–269. DOI: 10.1016/j.jhazmat.2004.10.028.
[8] World coal association, http://www.worldcoal.org, (2015).
[9] Durie, R.A., The Science of Victorian Brown Coal: structure, properties, and consequences for utilization, Butterworth-Heinemann, Oxford, (1991) 102–150.
[10] Gharebaghi, M., Irons, R.M.A., Jones, J. M., Pourkashanian, M., Williams, A., Study of effect of oxycoal combustion conditions on fly ash characteristics, Journal of the Energy Institute, 84 (2011) 155-164. DOI: 10.1179/174396711X13050315650787.
[11] Ramsdon, A.R., Shibaoka, M., Characterization and analysis of individual fly-ash particles from coal-fired power stations by a combination of optical microscopy, electron microscopy and quantitative electron microprobe analysis, Atmospheric Environment, (1982) 2191–2195. DOI: 10.1016/0004-6981(82)90290-6
[12] Sakorafa, V., Michailidis, K., Burragato, F., Mineralogy, geochemistry and physical properties of fly ash from the Megalopolis lignite fields, Peloponnese, southern Greece, Fuel, 75 (1996) 419– 423. DOI: 10.1016/0016-2361(95)00273-1.
[13] Pedersen, K.H., Jensen, A.D., Skjoth, R., Dam, J.K., A review of the interference of carbon containing fly ash with air entrainment in concrete, Progress in Energy and Combustion Science, 34 (2008) 135–154. DOI: 10.1016/j.pecs.2007.03.002.
[14] Kolay, P.K., Singh, D.N., Physical, chemical, mineralogical, and thermal properties of cenospheres from an ash lagoon, Cement and Concrete Research, 31 (2001) 539-542. DOI: 10.1016/S0008-8846(01)00457-4.
[15] Ngu, L., Wu, H., Zhang, D., Characterization of Ash Cenospheres in Fly Ash from Australian Power Stations, Energy Fuels, 21 (2007) 3437–3445. DOI: 10.1021/ef700340k.
[16] Kolay, P. K., Bhusal, S., Recovery of hollow spherical particles with two different densities from coal fly ash and their characterization, Fuel, 117 (2014) 118–124. DOI: 10.1016/j.fuel.2013.09.014.
[17] Raask, E., Hollow and spherical particles in pulverized-fuel ash, Journal of the institute of fuel, (1968) 339 – 344.
[18] Sokol, E.V., Maksimova, N.V., Volkova, N.I., Kalug, V.M., Nigmatulina, E.N., Frenkel, A.E., Hollow silicate microspheres from fly ashes of the Chelyabinsk brown coals (South Urals, Russia), Fuel Processing Technology, 67 (2000) 35–52. DOI: 10.1016/S0378-3820(00)00084-9.
[19] ASTM C 618, Standard specification for coal fly ash and raw or calcined natural pozzolan for use in concrete, ASTM International, (2015).
[20] Shaikh, F.U.A., Supit, S.W.M., Compressive strength and durability properties of high volume fly ash (HVFA) concretes containing ultrafine fly ash (UFFA), Construction and Building Materials, 82 (2015) 192–205. DOI:10.1016/j.conbuildmat.2015.02.068.
[21] Bendapudi S.C.K., Sasha, P., Contribution of fly ash to the properties of mortar and concrete, International Journal of Earth Sciences and Engineering, 4 (2011) 1017–1023.
[22] Metso expect results, Metso centrifugal classifier for fly ash processing, http://www.metso.com/miningandconstruction/MaTobox7.nsf/DocsByID/40C9FFFFCFFE2F8EC2257D8700462BB2/$File/FlyAshBrochure.pdf, (2016).
[23] Sturtevant, Inc., Air classifiers, http://www.sturtevantinc.com/products/air-classifiers/, (2016).
[24] Gloeckner, H., Hagemeier, T., Roloff, C., Thévenin, D., Tomas, J., Experimental Investigation on the Multistage Particle Classification in a Zigzag Air Classifier, Proceedings of the World Congress on Engineering, London, (2014).
[25] Petrus, H.T.B.M., Hirajima, T., Oosako, Y., Nonaka, M., Sasaki, K., Ando, T., Performance of dry-separation processes in the recovery of cenospheres from fly ash and their implementation in a recovery unit, International Journal of Mineral Processing, 98 (2011) 15–23. DOI: 10.1016/j.minpro.2010.09.002.
[26] Chindaprasirta, P., Homwuttiwong, S., Sirivivatnanon, V., Influence of fly ash fineness on strength, drying shrinkage and sulfate resistance of blended cement mortar, Cement and Concrete Research, 34 (2004) 1087 – 1092. DOI: 10.1016/j.cemconres.2003.11.021.
[27] Sinsiri, T., Teeramit, P., Jaturapitakkul, C., Kiattikomol, K., Effect of fineness of fly ash on expansion of mortars in magnesium sulfate, ScienceAsia, 32 (2006) 63–69, DOI: 10.2306/scienceasia1513-1874.2006.32.063.

[28] Termkhajornkita, P., Nawaa, T., Nakaib, M., Saito, T., Effect of fly ash on autogenous shrinkage, Cement and Concrete Research 35 (2005) 473 – 482, DOI: 10.1016/j.cemconres.2004.07.010.
[29] Kristiawana, S.A., Aditya, M.T.M, Effect of high volume fly ash on shrinkage of self-compacting concrete, Procedia Engineering 125 (2015) 705 – 712. DOI: 10.1016/j.proeng.2015.11.110.
[30] S. Tangtermsirikul, Effect of chemical composition and particle size of fly ash on autogenous shrinkage of paste, in: E. Tazawa (Ed.), Proceedings of the International Workshop on Autogenous Shrinkage of Concrete, JCI, Hiroshima, Japan, (1998) 175 – 186.
[31] Salber, A. J., Swan, C. W., Design of fly-ash concrete masonry for optimal carbon sequestration, World of coal ash (WOCA) conference, USA, (2013).
[32] Jones, M.R., McCarthy, A., Booth, A.P.P.G., Characteristics of the ultrafine component of fly ash, Fuel, 85 (2006) 2250–2259. DOI: 10.1016/j.fuel.2006.01.028.
[33] Rivera F., Martínez, P., Castro, J., Lopez, M., Massive volume fly-ash concrete: A more sustainable material with fly ash replacing cement and aggregates, Cement and Concrete Composites, 63 (2015) 104-112. DOI: 10.1016/j.cemconcomp.2015.08.001.
[34] V.M. Malhotra, P.K. Mehta, High-performance, High-volume Fly Ash Concrete for Building Sustainable and Durable Structures, third edition, ACCA, (2008).
[35] ČSN ISO 4013, Beton, Stanovení pevnosti v tahu ohybem zkušebních těles, Úřad pro technickou normalizaci, metrologii a státní zkušebnictví, Praha, (1994).
[36] ČSN ISO 1920, Zkoušení betonu. Rozměry, mezní odchylky a použití zkušebních těles, Úřad pro technickou normalizaci, metrologii a státní zkušebnictví, Praha, (1994).
[37] ČSN EN 480-1, Přísady do betonu, malty a injektážní malty - Zkušební metody - Část 1: Referenční beton a referenční malta pro zkoušení, Praha, (2015).
[38] ČSN EN 196-3, Metody zkoušení cementu - Část 3: Stanovení dob tuhnutí a objemové stálosti, Praha, (2005).
[39] ASTM C1202-12, Standard Test Method for Electrical Indication of Concrete's Ability to Resist Chloride Ion Penetration, ASTM International, West Conshohocken, PA, (2016).
[40] Horiba scientific, a guidebook to particle size analysis, https://www.horiba.com/fileadmin/uploads/Scientific/eMag/PSA/Guidebook/pdf/PSA_Guidebook.pdf, (2016).
[41] Hosokowa micron powder systems, http://www.hmicronpowder.com, (2016).
[42] Lu, Z., Huo, P., Luo, Y., Liu, X., Wu, D., Gao, X., Li, C., Yan, Y., Performance of molecularly imprinted photo catalysts based on fly-ash cenospheres for selective photo degradation of single and ternary antibiotics solution, Journal of Molecular Catalysis A: Chemical, 378 (2013) 91–98. DOI: 10.1016/j.molcata.2013.06.001.
[43] Hudak, P.F., Principles of hydrogeology, third edition, CRC Press LLC, (2005) 35-36.
[44] Chen, Y., Shah, N., Huggins, F.E., Huffman, G.P., Dozier, A., Characterization of ultrafine coal fly ash particles by energy-filtered TEM, Journal of Microscopy, 217 (2005) 225–234. DOI: 10.1111/j.1365-2818.2005.01445.x.
[45] Mindess, S., Young, J. F., Darwin, D., Concrete, Prentice Hall, Englewood Cliffs, NJ, USA, (2003).
[46] Delatte, N.J., Concrete pavement design, construction, and performance, second edition, CRC Press, Taylor & Francis Group, (2014).
[47] Chebet F.C., Kalumba, D., Laboratory Investigation on Re-Using Polyethylene (Plastic) Bag Waste Material for soil reinforcement in Geotechnical Engineering, Civil Engineering and Urban Planning: An International Journal (CiVEJ), 1 (2014).
[48] Lootens, D., Jousset, P., Martinie, L., Roussel, N., Flatt, R.J., Yield stress during setting of cement pastes from penetration tests, Cement and Concrete Research 39 (2009) 401–408. DOI:10.1016/j.cemconres.2009.01.012.
[49] Ravina, D., Slump retention of fly ash concrete with and without chemical admixtures, Concrete International, 17 (1995) 25-29.
[50] Liu, B., Xie, Y., Influence of fly ash on properties of cement – based materials, first international symposium on design, performance and use of self – consolidating concrete SCC, China, (2005). DOI: 10.1617/2912143624.060.